

## Synthesis and Magnetic Characterization of the Dioxo- and Oxohydroxo-bridged Dimeric Chromium(III) Cations Di- $\mu$ -oxobis[bis{1-(2-pyridyl)ethylamine}chromium(III)] and $\mu$ -oxo- $\mu$ -hydroxobis[bis{1-(2-pyridyl)ethylamine}chromium(III)], and Structure of the Bromide Salt of the Oxohydroxo Complex

KIRSTEN MICHELSEN, ERIK PEDERSEN

Chemistry Department I. Inorganic Chemistry, H. C. Ørsted Institute, University of Copenhagen, Universitetsparken 5, DK-2100 Copenhagen Ø, Denmark

SCOTT R. WILSON and DEREK J. HODGSON

Department of Chemistry, University of North Carolina, Chapel Hill, N.C. 27514, U.S.A.

Received May 4, 1982

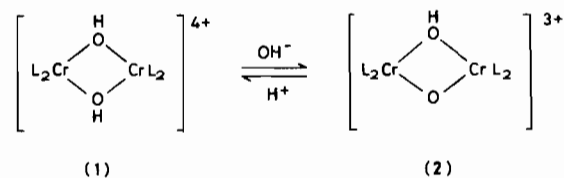
The syntheses of the title complex cations, di- $\mu$ -oxobis[bis{1-(2-pyridyl)ethylamine}chromium(III)],  $[(2\text{-picetam})_2\text{Cr}(\text{O})]_2^{2+}$  or  $[(\text{C}_7\text{H}_{10}\text{N}_2)_2\text{Cr}(\text{O})]_2^{2+}$ , and  $\mu$ -oxo- $\mu$ -hydroxobis[bis{1-(2-pyridyl)ethylamine}chromium(III)],  $[\text{Cr}_2(2\text{-picetam})_4(\text{OH})(\text{O})]^{3+}$  or  $[(\text{C}_7\text{H}_{10}\text{N}_2)_4\text{Cr}_2(\text{O})(\text{OH})]^{3+}$ , are reported, and their electronic and circular dichroism spectra in a variety of media are compared. The crystal and molecular structure of the  $\mu$ -oxo- $\mu$ -hydroxo complex as the bromide salt,  $[(2\text{-picetam})_4\text{Cr}_2(\text{O})(\text{OH})]\text{Br}_3 \cdot 5\text{H}_2\text{O}$ , has been determined from three-dimensional X-ray counter data. The complex crystallizes in the triclinic space group  $P\bar{1}$  with two binuclear complexes in a cell of dimensions  $a = 13.491(5)$ ,  $b = 13.762(3)$ ,  $c = 11.389(4)$  Å,  $\alpha = 104.41(2)$ ,  $\beta = 106.39(3)$ , and  $\gamma = 84.44(2)^\circ$ . Least-squares refinement of the structure using 2969 independent intensities has yielded a weighted R-factor (on F) of 0.052. The cation consists of two roughly octahedral chromium(III) centers, with terminal Cr–N distances in the range 2.057(5)–2.130(6) Å. The Cr–Cr separation is 2.833(2) Å, and the bridging Cr–O–Cr angles at the oxo and hydroxo oxygen atoms are  $100.6(2)^\circ$  and  $95.0(2)^\circ$ , respectively. The Cr–O distances to the oxo oxygen atom are 1.869(4) and 1.878(4) Å, while those to the hydroxo bridge are 1.960(4) and 1.950(4) Å. The magnetic susceptibility of this  $\mu$ -oxo-hydroxo complex shows a maximum near 100 K. A fit of the data to a model assuming independent triplet, quintet, and septet energies is almost consistent with the Heisenberg model corrected for biquadratic exchange, and leads to a triplet energy of  $46.45(2)$   $\text{cm}^{-1}$ . In the di- $\mu$ -oxo complex, examined

as the chloride salt, the triplet energy is approximately  $83$   $\text{cm}^{-1}$ .

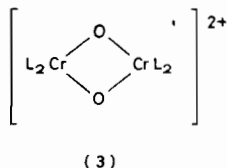
### Introduction

The spectral, structural, and magnetic properties of dimeric chromium(III) complexes continue to be the subjects of intense research activity [1–12]. For the di- $\mu$ -hydroxo dimers  $[\text{CrL}_2\text{OH}]_2^{n+}$  it has been noted that the sign and magnitude of the isotropic exchange coupling parameter for the ground states (J) depends on the Cr–O–Cr bridging angle ( $\phi$ ) [2,3,8,10,13–15], the Cr–O bridging bond length (R) [2,8,14,15], and the dihedral angle between the bridging  $\text{Cr}_2\text{O}_2$  plane and the O–H vector ( $\theta$ ) [1–3, 12, 16]; very recently we have derived a quantitative relationship between J and these three structural parameters for this class of complexes [15, 17]. We intend to extend the model to other complexes, including the singly hydroxo-bridged dimers,  $[\text{L}_5\text{Cr}(\text{OH})\text{CrL}_5]^{n+}$ , [5, 10, 12].

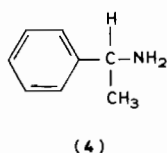
The existence of the pH-dependent equilibrium between the di- $\mu$ -hydroxo (1) and the  $\mu$ -oxo- $\mu$ -hydroxo (2) complexes is well established [18], and this and related equilibria have been exploited



by Springborg and coworkers [6]. We have now bromide salt of 2,  $\mu$ -oxo- $\mu$ -hydroxobis [bis{1-(2-



and di- $\mu$ -oxo (3) species of a single system where L is 1-(2-pyridyl)ethylamine (4) [19]. The synthesis and spectral and magnetic properties of the di- $\mu$ -hydroxo complex (1) have been described previously [1],



and the crystal structure of a salt of this complex has been determined [20]. We here report the synthesis and spectral and magnetic properties of complexes 2 and 3, and the crystal structure of the bromide salt of 2,  $\mu$ -oxo- $\mu$ -hydroxobis [bis{1-(2-pyridyl)ethylamine}chromium(III)] bromide pentahydrate,  $[\text{Cr}_2(2\text{-picetam})_4(\text{OH})(\text{O})]\text{Br}_3 \cdot 5\text{H}_2\text{O}$ .

## Experimental

### Reagents

Racemic di- $\mu$ -hydroxobis[bis-1-(2-pyridyl)ethylamine chromium(III)] bromide trihydrate was prepared and resolved as described before [1]. SP-Sephadex C 25 was purchased from Pharmacia, Uppsala, Sweden. All other chemicals were of reagent grade and were used without further purifications.

### Analyses

The chromium analyses were performed on a Perkin Elmer 403 Atomic Absorption Spectrophotometer. The microanalytical laboratory of the H. C. Ørsted Institute in Copenhagen carried out the carbon, nitrogen, hydrogen and halogen analyses by standard methods.

### Syntheses

$\mu$ -oxo- $\mu$ -hydroxobis[bis{1-(2-pyridyl)ethylamine}chromium(III)] bromide pentahydrate,  $[(\text{C}_7\text{H}_{10}\text{N}_2)_2\text{Cr}(\text{O})(\text{OH})\text{Cr}(\text{C}_7\text{H}_{10}\text{N}_2)_2]\text{Br}_3 \cdot 5\text{H}_2\text{O}$   
 $[(\text{C}_7\text{H}_{10}\text{N}_2)_2\text{Cr}(\text{OH})_2\text{Cr}(\text{C}_7\text{H}_{10}\text{N}_2)_2]\text{Br}_4 \cdot 3\text{H}_2\text{O}$   
 (0.3 g, 0.30 mmol) was dissolved in boiling water (2 ml). 2 M sodium hydroxide (1 ml) was added, and the solution was heated for a few seconds. After-

wards the solution was left for some hours at room temperature in a covered beaker. After that time large, olive-green crystals had separated. They were filtered, washed with ethanol-ether (1:1) and with ether. The yields from different experiments ranged from 0.254 g to 0.180 g (89%–63%). (Found: Cr 10.85; C 34.96; N 11.69; H 4.76; Br 24.99. Calc. for  $[\text{Cr}_2(\text{O})(\text{OH})(\text{C}_7\text{H}_{10}\text{N}_2)_4]\text{Br}_3 \cdot 5\text{H}_2\text{O}$ : Cr 10.88; C 35.19; N 11.73; H 5.38; Br 25.08).

$(-)_D$ - $\mu$ -oxo- $\mu$ -hydroxobis[bis{1-(2-pyridyl)ethylamine}chromium(III)] bromide nonahydrate,  
 $(-)_D$ - $[(\text{C}_7\text{H}_{10}\text{N}_2)_2\text{Cr}(\text{O})(\text{OH})\text{Cr}(\text{C}_7\text{H}_{10}\text{N}_2)_2]\text{Br}_3 \cdot 9\text{H}_2\text{O}$

The compound was prepared as above except that the starting material, the racemic diol, was replaced by the corresponding optically active diol. Yields ~ 50%. (Found: C 32.73; N 11.00; H 4.95; Br 22.88. Calc. for  $(-)_D$ - $[\text{Cr}_2(\text{O})(\text{OH})(\text{C}_7\text{H}_{10}\text{N}_2)_4]\text{Br}_3 \cdot 9\text{H}_2\text{O}$ : C 32.83; N 10.91; H 5.80; Br 23.40).

*Di- $\mu$ -oxo-bis[bis{1-(2-pyridyl)ethylamine}chromium(III)] chloride octahydrate,  $[(\text{C}_7\text{H}_{10}\text{N}_2)_2\text{Cr}(\text{O})_2\text{Cr}(\text{C}_7\text{H}_{10}\text{N}_2)_2]\text{Cl}_2 \cdot 8\text{H}_2\text{O}$*

The starting material,  $[(\text{C}_7\text{H}_{10}\text{N}_2)_2\text{Cr}(\text{OH})_2\text{Cr}(\text{C}_7\text{H}_{10}\text{N}_2)_2]\text{Cl}_4 \cdot 2\text{H}_2\text{O}$  was prepared from the corresponding bromide by ion exchange. The bromide was absorbed on a column of an SP-Sephadex C-25 cation exchanger. Elution with 0.1 M hydrochloric acid removed the bromide ions. The diol was eluted afterwards with 4 M hydrochloric acid and precipitated with ethanol and ether.

$[(\text{C}_7\text{H}_{10}\text{N}_2)_2\text{Cr}(\text{OH})_2\text{Cr}(\text{C}_7\text{H}_{10}\text{N}_2)_2]\text{Cl}_4 \cdot 2\text{H}_2\text{O}$   
 (0.35 g, 0.42 mmol) was dissolved in hot water (1 ml). 4 M sodium hydroxide (2 ml) was added, and the solution was allowed to stand in a covered beaker for some hours. At that time large brown-yellow crystals had separated. They were filtered and washed with ethanol-ether (1:1) and with ether. The yields from different experiments ranged from 0.208–0.140 g (59–40%). (Found: Cr 12.41; C 40.05; N 13.28; H 5.87; Cl 8.55. Calc. for  $[\text{Cr}_2(\text{O})_2(\text{C}_7\text{H}_{10}\text{N}_2)_4]\text{Cl}_2 \cdot 8\text{H}_2\text{O}$ : Cr 12.39; C 40.05; N 13.35; H 6.72; Cl 8.44).

### Physical Measurements

Absorption spectra were recorded on a Cary Model 14 and a Cary Model 118 spectrophotometer. Circular Dichroism was measured on a Roussel-Jouan Dichrographe III,  $[\text{Coen}_3]\text{Cl}_3 \cdot \frac{1}{2}\text{NaCl} \cdot 3\text{H}_2\text{O}$  being used as a standard, (1.92, 489). Racemic and optically active di- $\mu$ -hydroxobis[bis{1-(2-pyridyl)ethylamine}chromium(III)] bromide trihydrate was dissolved in 0.1 M hydrochloric acid, 0.1 M sodium hydroxide + 0.9 M sodium chloride, 4 M sodium hydroxide and a solution of lithium methoxide in ethanol (vis. region only). The different media were chosen in order to obtain spectra of the di- $\mu$ -

hydroxo ion, the  $\mu$ -oxo- $\mu$ -hydroxo ion and the di- $\mu$ -oxo ion, respectively. The acid dissociation constant  $K_{a1}$  of the di- $\mu$ -hydroxo ion was determined roughly by Ole Mønsted; a more detailed description of the potentiometric method and of the equipment is published elsewhere [21]. The preliminary result is  $pK_{a1} = 10.7$ ,  $\mu = 1 M$ ,  $25^\circ C$ .

### Magnetic Measurements

The magnetic susceptibilities of microcrystalline samples were measured by the Faraday method at a field strength of 12000 Oe in the temperature range 2–300 K. Preliminary descriptions of the instrumentation are found elsewhere [2].

### Crystallographic Measurements

A translucent crystal of the bromide salt of 2,  $[(C_7H_{10}N_2)_4Cr_2(OH)(O)]Br_3 \cdot 5H_2O$ , was mounted on an Enraf-Nonius automated X-ray diffractometer; preliminary analysis indicated that the crystals belong to the triclinic system, the space group being either  $C_1^1-P1$  or  $C_1^1-P\bar{1}$ . The centrosymmetric space group ( $P\bar{1}$ ) was chosen, and this selection was verified by the successful refinement of the structure. Cell constants determined from a least-squares fit of the diffractometer settings of 25 reflections were  $a = 13.491(5)$ ,  $b = 13.762(3)$ ,  $c = 11.389(4)$  Å,  $\alpha = 104.41(2)$ ,  $\beta = 106.39(3)$ ,  $\gamma = 84.44(2)^\circ$ ; the observations were made at 22°C using  $MoK\alpha$  radiation and an assumed wavelength of 0.7107 Å. A density of  $1.615 g cm^{-3}$  calculated for two (binuclear) formula units per cell is in good agreement with the value of  $1.59(2) g cm^{-3}$  measured by flotation in chloroform/1,3-dibromopropane mixture; hence, in space group  $P\bar{1}$ , no crystallographic symmetry is imposed on the molecule.

Diffraction data were collected from a prismatic crystal mounted roughly parallel to the crystallographic  $b$ -axis. The data were collected in the manner described elsewhere [22] on an Enraf-Nonius CAD4-SDP diffractometer equipped with a molybdenum tube and a graphite monochromator. The data were corrected for background counts and were assigned estimated standard deviations,  $\sigma(I)$ , on the basis of counting statistics. The values of  $I$  and  $\sigma(I)$  were corrected for Lorentz-polarization effects and for absorption. The linear coefficient for these atoms with  $MoK\alpha$  radiation is  $38.6 cm^{-1}$ , and for the crystal chosen the application of a numerical absorption correction gave minimum and maximum transmission coefficients of 0.36 and 0.45, respectively, with an average value of 0.42. There were 2969 independent data whose intensities exceeded three times their estimated standard deviations; only these data were used in the subsequent structure analysis.

### Solution and Refinement of the Structure

The structure was solved by direct methods, using the multiple solution program MULTAN [23]. A set of 359 normalized structure amplitudes was used as input, and 32 solutions were generated. The chosen solution revealed the positions of the three bromine and two chromium atoms as the top five peaks in an E-map. Isotropic least-squares refinement of these positions yielded values of the conventional agreement factors  $R_1 = \sum ||F_o| - |F_c|| / \sum |F_o|$  and  $R_2 = [\sum w(|F_o| - |F_c|)^2 / \sum w(F_o)^2]^{1/2}$  of 0.367 and 0.457, respectively. All least-squares refinements were carried out on  $F$ , the function minimized being  $w(|F_o| - |F_c|)^2$ ; the weights,  $w$ , were taken as  $4F_o^2 / \sigma^2(F_o)^2$ , where  $\sigma(F_o)^2$  is given by  $[\sigma^2(I) + p^2 I^2]^{1/2}$  and the parameter  $p$  was set to 0.01 [24]. Subsequent difference Fourier syntheses revealed the locations of the 43 remaining non-hydrogen atoms, and isotropic refinement of all 48 atoms gave values of 0.072 and 0.095 for  $R_1$  and  $R_2$ , respectively. The positions of all hydrogen atoms which could be calculated on the basis of anticipated geometries at C or N were constrained to their calculated values; these geometries were based on C–H and N–H distances of 0.95 and 0.90 Å, respectively [25], and tetrahedral or trigonal geometry as appropriate. The hydrogen atom attached to the bridging hydroxyl oxygen atom [O(2)] was located in a difference Fourier map and was constrained to this observed position. Since none of the hydrogen atoms associated with the five water molecules could be identified in a difference Fourier map, their contribution to  $F_c$  was excluded. All other hydrogen atoms were assigned fixed isotropic thermal parameters of  $1.5 \text{ \AA}^2$  greater than the isotropic thermal parameter of the atom to which they were attached [22]. The final least-squares calculation, which involved anisotropic refinement of all non-hydrogen atom parameters, gave values for  $R_1$  and  $R_2$  of 0.056 and 0.052, respectively; in the final cycle, no parameter experienced a shift in excess of  $0.1\sigma$ , which is taken as evidence of convergence. A final difference Fourier map contained numerous peaks in the range 0.25 to  $0.56 e\text{\AA}^{-3}$  but revealed no chemically meaningful features. No correction for secondary extinction appeared necessary. The atomic positional parameters, along with their standard deviations as estimated from the inverse matrix, are listed in Table I. Listings of anisotropic librational parameters and of observed and calculated structure amplitudes are available from the editor as supplementary material.

### Results and Discussion

#### Spectroscopic Study

The absorption and circular dichroism spectra of  $(-)_D-[Cr(2\text{-picetam})_2OH]_2Br_4 \cdot 3H_2O$  in different

TABLE I. Positional Parameters for  $[\text{Cr}_2(2\text{-picetam})_4\text{-(OH)O}]\text{Br}_3\cdot 5\text{H}_2\text{O}$ .<sup>a</sup>

Atom	X	Y	Z
Br1	0.6706(1)	0.95781(9)	0.1820(1)
Br2	0.6270(1)	0.66244(11)	0.4159(1)
Br3	0.8314(1)	0.60675(10)	-0.0637(1)
Cr1	0.1436(1)	0.7551(1)	0.0596(1)
Cr2	0.3469(1)	0.8269(1)	0.0993(1)
O1	0.2071(4)	0.8615(4)	0.0372(5)
O2	0.2874(5)	0.7112(4)	0.1215(5)
O1W	0.8859(5)	0.9866(5)	0.0571(6)
O2W	0.4024(6)	0.6138(5)	0.3221(6)
O3W	0.8585(6)	0.7536(7)	0.4336(7)
O4W	0.8578(7)	0.7871(7)	0.1978(8)
O5W	0.6929(10)	0.5413(7)	-0.3597(9)
NA	0.1313(6)	0.6655(6)	-0.1179(7)
NA'	-0.0005(6)	0.7969(5)	-0.0384(7)
NB	0.1206(6)	0.8317(6)	0.2319(7)
NB'	0.0869(6)	0.6414(6)	0.1155(7)
NC	0.3606(6)	0.9115(6)	0.2806(6)
NC'	0.3966(6)	0.9633(6)	0.0915(6)
ND	0.3669(6)	0.7554(6)	-0.0765(7)
ND'	0.4992(6)	0.7632(6)	0.1464(7)
CA2	0.0577(7)	0.6910(7)	-0.2128(8)
CA3	0.0454(8)	0.6409(7)	-0.3357(9)
CA4	0.1104(8)	0.5583(8)	-0.3604(9)
CA5	0.1834(8)	0.5281(7)	-0.2636(9)
CA6	0.1930(8)	0.5834(7)	-0.1447(9)
CA2'	-0.0035(8)	0.7836(8)	-0.1717(9)
CA3'	-0.1130(9)	0.7889(9)	-0.2541(10)
CB2	0.1091(8)	0.7749(7)	0.3082(8)
CB3	0.1018(8)	0.8175(8)	0.4272(9)
CB4	0.1028(8)	0.9211(9)	0.4673(9)
CB5	0.1100(8)	0.9778(8)	0.3882(9)
CB6	0.1194(8)	0.9316(7)	0.2726(9)
CB2'	0.1140(8)	0.6626(8)	0.2543(9)
CB3'	0.0533(12)	0.6046(9)	0.3001(11)
CC2	0.3616(7)	1.0133(7)	0.2942(8)
CC3	0.3636(8)	1.0782(8)	0.4069(9)
CC4	0.3651(8)	1.0413(8)	0.5079(9)
CC5	0.3687(8)	0.9386(8)	0.4946(8)
CC6	0.3669(7)	0.8769(7)	0.3818(8)
CC2'	0.3556(8)	1.0454(7)	0.1757(8)
CC3'	0.4067(9)	1.1417(8)	0.1949(10)
CD2	0.4464(8)	0.6879(7)	-0.0774(9)
CD3	0.4653(9)	0.6358(8)	-0.1887(10)
CD4	0.4087(10)	0.6544(9)	-0.2984(10)
CD5	0.3262(9)	0.7246(8)	-0.2979(9)
CD6	0.3091(8)	0.7727(7)	-0.1855(9)
CD2'	0.5072(9)	0.6722(9)	0.0511(10)
CD3'	0.6076(12)	0.6290(11)	0.0611(13)

<sup>a</sup>Hydrogen atom parameters, which were not refined, are available as supplementary material.

media are presented in Figs. 1–4 and are summarized in Tables II and III. Since the spectra of this di- $\mu$ -hydroxo complex (I) in 0.01 M HCl do not detectably change within 24 hours, we may safely

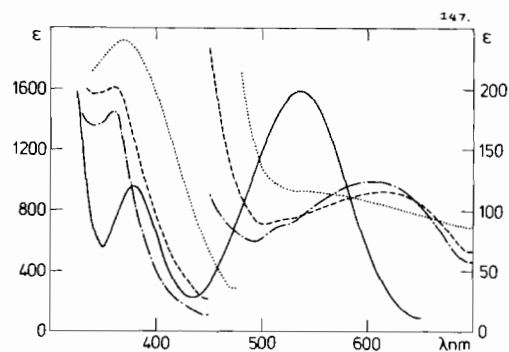


Fig. 1. The absorption spectra of  $[(\text{C}_7\text{H}_{10}\text{N}_2)_2\text{Cr}(\text{OH})_2\text{-Cr}(\text{C}_7\text{H}_{10}\text{N}_2)_2]\text{Br}_4\cdot 3\text{H}_2\text{O}$  in 0.1 M HCl (—), in 0.1 M NaOH + 0.9 M NaCl (---), in 4 M NaOH (-.-.-) and in LiOMe–Ethanol (.....). Region 700–350 nm.

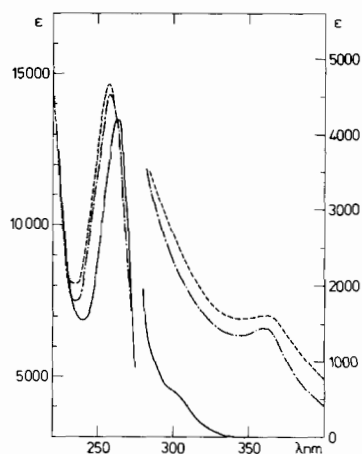


Fig. 2. The absorption spectra of  $[(\text{C}_7\text{H}_{10}\text{N}_2)_2\text{Cr}(\text{OH})_2\text{-Cr}(\text{C}_7\text{H}_{10}\text{N}_2)_2]\text{Br}_4\cdot 3\text{H}_2\text{O}$  in 0.1 M HCl (—), in 0.1 M NaOH + 0.9 M NaCl (---), and in 4 M NaOH (-.-.-). Region 400–220 nm.

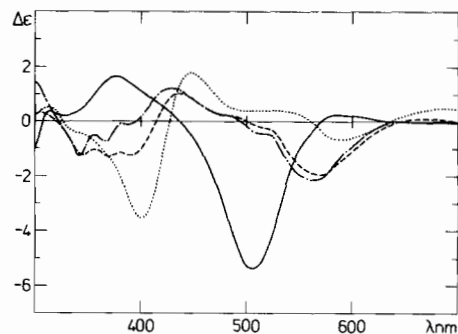


Fig. 3. The circular dichroism spectra of  $[(-)\text{-D-}[(\text{C}_7\text{H}_{10}\text{N}_2)_2\text{Cr}(\text{OH})_2\text{-Cr}(\text{C}_7\text{H}_{10}\text{N}_2)_2]\text{Br}_4\cdot 3\text{H}_2\text{O}$  in 0.1 M HCl (—), in 0.1 M NaOH + 0.9 M NaCl (---), in 4 M NaOH (-.-.-) and in LiOMe–Ethanol (.....). 700–300 nm.

TABLE II. Electronic Spectral Parameters for Di- $\mu$ -hydroxobis[bis{1-(2-pyridyl)ethylamine}chromium(III)] Bromide Trihydrate in Different Media. Region 700–300 nm. L = 1-2(pyridyl)ethylamine.

Medium	Ion, presumed to be dominant	$\lambda_{\max}$ nm	$\epsilon_{\max}$
0.1 M HCl	$[\text{L}_2\text{Cr}(\text{OH})_2\text{CrL}_2]^{4+}$	535.5	199
		378	120
0.1 M NaOH + 0.9 M NaCl	$[\text{L}_2\text{Cr}(\text{O})(\text{OH})\text{CrL}_2]^{3+}$	610	124
		360	1451
LiOMe in ethanol	$[\text{L}_2\text{Cr}(\text{O})_2\text{CrL}_2]^{2+}$	~550 sh	~116
		370	1924

TABLE III. CD-Spectral Parameters for (-)<sub>D</sub>Di- $\mu$ -hydroxobis[bis{1-(2-pyridyl)ethylamine}chromium(III)] Bromide Trihydrate in Different Media. Region 700–300 (297) nm. L = 1-2(pyridyl)ethylamine.

Medium	Ion, presumed to be dominant	$\lambda_{\text{ex}}$ nm	$\Delta\epsilon_{\text{ex}}$
0.1 M HCl	$[\text{L}_2\text{Cr}(\text{OH})_2\text{CrL}_2]^{4+}$	586	+0.25
		505	-5.36
		377	+1.66
		314	+0.37
		297	-1.27
0.1 M NaOH	$[\text{L}_2\text{Cr}(\text{O})(\text{OH})\text{CrL}_2]^{3+}$	659	+0.09
		566	-2.13
		512	-0.46
		474	+0.28
		433	+1.22
		388	-0.13
		368	-0.74
LiOMe in ethanol	$[\text{L}_2\text{Cr}(\text{O})_2\text{CrL}_2]^{2+}$	343	-1.27
		684	+0.48
		588	-0.67
		525	+0.41
		449	+1.77
	402	-3.53	
	315	+0.55	

assume that (1) does not equilibrate rapidly with the corresponding  $\mu$ -hydroxo complex; such equilibration is observed in the analogous ethylenediamine complexes [6c]. The visible absorption spectra of (1) in water, 0.1 M HCl, and 1.0 M HCl are identical and resemble the spectrum of the racemic di- $\mu$ -hydroxo-chromium(III) complex with ethylenediamine [6c].

We may also conclude that a solution of (1) in 0.1 M NaOH + 0.9 M NaCl contains a single species, namely the  $\mu$ -oxo- $\mu$ -hydroxo ion (2). The spectra do not appear to change within 24 hours, and the visible absorption spectrum is entirely different from that of the dihydroxo- $\mu$ -hydroxo complex with ethylenediamine [6c]. A solution of (-)<sub>D</sub>[Cr<sub>2</sub>(2-picetam)<sub>4</sub>-

(OH)(O)]Br<sub>3</sub> in DMF gave a visible CD spectrum of the same general appearance, with only slightly different intensities. In Figs. 1–4 are also shown the spectra of (1) dissolved in 4 M NaOH. These spectra evidently result from a mixture of (2) (major component) and the di- $\mu$ -oxo complex (3) (minor component).

To obtain the visible spectra of (3) we dissolved (1) in an ethanol solution of lithium methoxide. This strongly basic solution is yellow, like the solid sample of (3), and presumably contains (3) as the major component. The X-ray analysis [20] of (+)<sub>D</sub>-{[(S)(-)<sub>D</sub>-C<sub>7</sub>H<sub>10</sub>N<sub>2</sub>]<sub>2</sub>Cr(OH)<sub>2</sub>Cr{(S)(-)<sub>D</sub>-C<sub>7</sub>H<sub>10</sub>N<sub>2</sub>]<sub>2</sub>}(S<sub>2</sub>O<sub>6</sub>)<sub>2</sub>·2H<sub>2</sub>O} proves that this compound

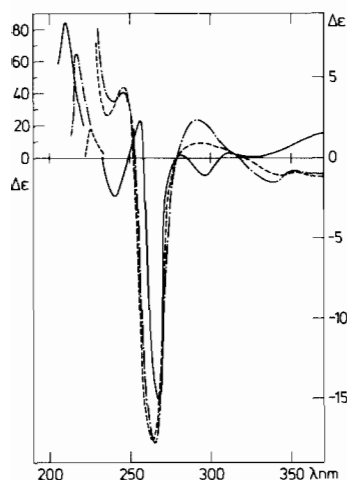


Fig. 4. The circular dichroism spectra of  $(-)\text{-D-}[(\text{C}_7\text{H}_{10}\text{N}_2)_2\text{-Cr}(\text{OH})_2\text{Cr}(\text{C}_7\text{H}_{10}\text{N}_2)_2]\text{Br}_4 \cdot 3\text{H}_2\text{O}$  in 0.1 M HCl (—), in 0.1 M NaOH + 0.9 M NaCl (---), and in 4 M NaOH (- - -). Region 350–200 nm.

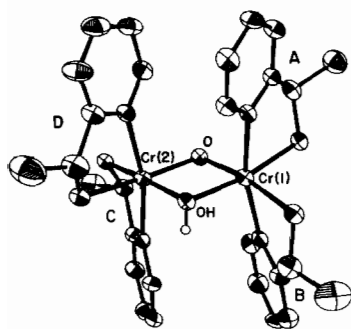


Fig. 5. View of the binuclear cation  $[\text{Cr}(\text{2-picetam})_2(\text{OH})(\text{O})\text{-Cr}(\text{2-picetam})_2]^{3+}$ . The dimer shown here exhibits the  $\Delta\Delta$  configuration.

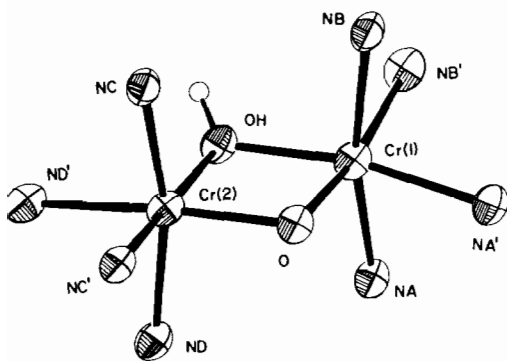


Fig. 6. View of the coordination around the chromium(III) centers in  $[\text{Cr}(\text{2-picetam})_2(\text{OH})(\text{O})\text{Cr}(\text{2-picetam})_2]^{3+}$ .

has the configuration  $\Lambda\Lambda$ . The catoptromer, whose circular dichroism spectrum (vis. region) is shown in Fig. 3 consequently has the configuration  $\Delta\Delta$ . This

TABLE IV. Internuclear Distances (Å) and Angles ( $^\circ$ ) for the Inner Coordination Spheres in 2.

Atoms	Distance	Atoms	Distance
Cr1–O1	1.869(4)	Cr2–O1	1.878(4)
Cr1–O2	1.960(4)	Cr2–O2	1.950(4)
Cr1–NA	2.060(6)	Cr2–NC	2.069(5)
Cr1–NA'	2.057(5)	Cr2–NC'	2.084(5)
Cr1–NB	2.076(6)	Cr2–ND	2.079(6)
Cr1–NB'	2.107(5)	Cr2–ND'	2.130(6)
NA–NA'	2.593(8)	NC–NC'	2.608(7)
NB–NB'	2.643(8)	ND–ND'	2.642(8)
Cr1–Cr2	2.883(2)	O2–H2	0.90

Atoms	Angle	Atoms	Angle
O1–Cr1–O2	82.2(2)	O1–Cr2–O2	82.2(2)
O1–Cr1–NA	96.3(2)	O1–Cr2–NC	95.4(2)
O1–Cr1–NA'	92.9(2)	O1–Cr2–NC'	92.8(2)
O1–Cr1–NB	94.8(2)	O1–Cr2–ND	94.6(2)
O1–Cr1–NB'	170.6(2)	O1–Cr2–ND'	169.9(2)
O2–Cr1–NA	92.4(2)	O2–Cr2–NC	95.7(2)
O2–Cr1–NA'	168.8(2)	O2–Cr2–NC'	171.5(2)
O2–Cr1–NB	97.6(2)	O2–Cr2–ND	94.6(2)
O2–Cr1–NB'	92.3(2)	O2–Cr2–ND'	91.8(2)
NA–Cr1–NA'	78.1	NC–Cr2–NC'	77.8(2)
NA–Cr1–NB	165.9(2)	NC–Cr2–ND	166.5(2)
NA–Cr1–NB'	91.5(2)	NC–Cr2–ND'	93.2(2)
NA'–Cr1–NB	92.8(2)	NC'–Cr2–ND	92.7(2)
NA'–Cr1–NB'	93.8(2)	NC'–Cr2–ND'	94.1(2)
NB–Cr1–NB'	78.4(2)	ND–Cr2–ND'	77.8(3)
Cr1–NA–CA2	117.1(5)	Cr2–NC–CC2	115.0(4)
Cr1–NA–CA6	124.6(5)	Cr2–NC–CC6	126.6(5)
Cr1–NA'–CA2'	109.7(4)	Cr2–NC'–CC2'	109.5(4)
Cr1–NB–CB2	116.5(5)	Cr2–NC–CD2	116.2(5)
Cr1–NB–CB6	124.7(5)	Cr2–NC–CD6	125.1(5)
Cr1–NB'–CB2'	109.5(4)	Cr2–ND'–CD2'	109.3(5)
Cr1–O1–Cr2	100.6(2)	Cr2–O2–Cr1	95.0(2)
Cr1–O2–H2	122.9	Cr2–O2–H2	128.4

is in agreement with the empirical rule that relates a dominant negative CD-band in the region of the cubic  ${}^4\text{A}_{2g} \rightarrow {}^4\text{T}_{2g}$  d–d absorption of the chromium(III) ion to a  $\Delta\Delta$  configuration [26]. The rule, however, does not seem very suitable for use on ions of the same type as the  $(-)\text{-D-}\mu\text{-oxo-}\mu\text{-hydroxo-}$  and the  $(-)\text{-D-}\mu\text{-di-}\mu\text{-oxoions}$ . Circular dichroism spectra of this type of basic species have never been reported before. In forthcoming publications we will present spectra of similar compounds with related ligands and show that they have the same characteristic appearance.

#### Description of the Structure of 2

The structure consists of binuclear  $[\text{Cr}_2(\text{2-picetam})_4(\text{O})(\text{OH})]^{3+}$  cations, bromide anions, and water molecules which are hydrogen bonded to each other in the crystal. A view of the binuclear cation is given

TABLE V. Internuclear Distances (Å) and Angles (°) for the Four 1-(2-Pyridyl)ethylamine Ligands in 2.

Atoms	Ligand				
	A	B	C	D	Average
Distances (Å)					
N–C2	1.339(7)	1.352(8)	1.372(8)	1.350(8)	1.353(14)
N–C6	1.360(8)	1.337(8)	1.332(7)	1.331(8)	1.340(14)
C2–C3	1.368(9)	1.363(9)	1.364(9)	1.371(10)	1.367(4)
C2–C2'	1.497(9)	1.517(9)	1.500(9)	1.519(10)	1.508(11)
C3–C4	1.388(9)	1.385(10)	1.362(10)	1.339(10)	1.369(23)
C4–C5	1.376(9)	1.357(10)	1.380(10)	1.401(11)	1.379(18)
C5–C6	1.356(9)	1.348(9)	1.347(9)	1.359(9)	1.353(6)
C2'–C3'	1.515(9)	1.468(10)	1.492(9)	1.411(11)	1.472(45)
C2'–N'	1.473(8)	1.478(8)	1.463(7)	1.457(9)	1.468(10)
Angles (°)					
C2–N–C6	118.4(6)	118.8(6)	118.4(6)	118.7(6)	118.6(2)
N–C2–C3	122.7(7)	121.2(2)	121.2(6)	120.7(7)	121.5(9)
N–C2–C2'	113.3(6)	114.6(7)	114.7(6)	115.0(7)	114.4(8)
C3–C2–C2'	123.8(7)	124.0(8)	124.1(7)	124.2(8)	124.0(2)
C2–C3–C4	117.6(7)	118.5(7)	119.4(7)	120.8(8)	119.1(14)
C3–C4–C5	120.6(7)	120.0(7)	118.9(7)	118.7(8)	119.6(9)
C4–C5–C6	118.3(7)	118.9(8)	119.9(7)	118.3(8)	118.9(8)
N–C6–C5	122.3(7)	122.5(7)	122.1(7)	122.7(7)	122.7(6)
C2–C2'–C3'	114.8(7)	114.0(7)	114.9(6)	116.9(8)	115.2(12)
C2–C2'–N'	109.8(6)	109.9(6)	108.6(6)	109.1(7)	109.4(6)
C3'–C2'–N'	112.1(6)	112.5(7)	111.5(6)	115.4(8)	112.9(17)

in Fig. 5, and the inner coordination sphere of the two chromium centers is depicted in Fig. 6. The bond lengths and bond angles in the inner sphere are listed in Table IV, while those in the four 2-picetam ligands are documented in Table V. As can be seen in Fig. 6, the geometry around each chromium(III) center is roughly octahedral, the ligating atoms being two pyridine nitrogen and two amine nitrogen atoms from the 2-picetam ligands and the two oxygen atoms from the bridging oxo and hydroxo ligands. There are, of course, considerable angular distortions from idealized octahedral geometry, the *cis* angles varying from 78.4 to 97.6° at Cr(1) and 77.8 to 95.7° at Cr(2) and the *trans* angles from 165.9 to 170.6° and from 166.5 to 171.5° at Cr(1) and Cr(2), respectively.

The Cr–N distances are in the range 2.057(5)–2.130(6) Å, the two largest values being associated with the Cr–N bonds which are *trans* to the oxo ligand. In the dihydroxo complex [20], the Cr–N distances are 2.048(5)–2.068(5) Å, which is comparable to the range of 2.057(5)–2.084(5) Å found here for the six shortest bonds and may be in contrast to the values of 2.107(5) and 2.130(6) Å for the Cr(1)–NB' and Cr(2)–ND' bonds, respectively.

These data, therefore, may suggest the presence of a significant *trans* effect of the oxo ligand. Similarly, the two Cr–OH separations of 1.960(4) and 1.950(4) Å are comparable to the values of 1.943(4)–1.947(4) Å in (I) [20] and to the values reported in numerous other hydroxo-bridged complexes of chromium(III), [3–5, 7, 10–12, 15] but the Cr–O distances of 1.869(4) and 1.878(4) Å to the oxo ligands are significantly shorter than these other values, and even approach the value of 1.815(1) Å found [27] in the linear oxo-bridged basic rhodo complex,  $[(\text{NH}_3)_5\text{Cr}(\text{O})\text{Cr}(\text{NH}_3)_5]^{4+}$ . Moreover, this Cr–O bond length is *shorter* than the values of approximately 1.89 Å in the di- $\mu$ -oxo complex, 3 [30]. The Cr(1)–Cr(2) separation of 2.883(2) Å is substantially shorter than the value of 3.021(1) Å in the dihydroxo complex [20], and is shorter than the Cr–Cr separation in any dihydroxo-bridged dimer whose structure has been reported, which are in the range 2.950–3.059 Å [3, 4, 7, 11, 15, 20]. The bridging Cr–O–Cr angles at the oxo and hydroxo atoms are 100.6(2)° and 95.0(2)°; this latter value is again smaller than the range of 97.6–103.4° found in the dihydroxo complexes.

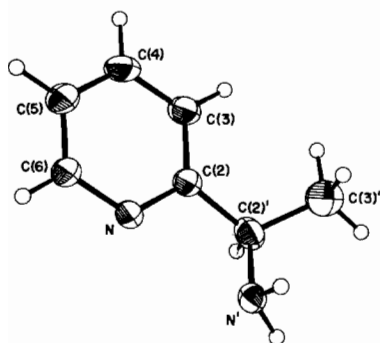


Fig. 7. Schematic drawing of the 1-(2-pyridyl)ethylamine, 2-picetam, ligand illustrating the atomic labeling.

The  $\text{Cr}_2\text{O}_2$  bridging unit is significantly non-planar, although none of the four atoms deviates from the least-squares plane by more than 0.013 Å. The hydrogen atom on the hydroxo group is apparently 0.43 Å out of this plane, which corresponds to a  $\theta$  angle of  $28.6^\circ$ . Since the hydrogen position was not refined, however, it would be dangerous to attach much significance to this parameter.

The stereochemistry of the binuclear cation can be seen in Fig. 5. The absolute configuration of the binuclear complex shown is  $\Delta\Delta$ , but in this centrosymmetric crystal there is an equal number of cations with the  $\Lambda\Lambda$  configuration. As was the case for the dihydroxo-bridged complex and was predicted earlier [1], the isomer studied here is the one with the pyridine nitrogen atoms *trans* to each other and

(therefore) occupying the apical positions. Of the fourteen theoretically possible  $\Delta\Delta$  and  $\Lambda\Lambda$  isomers, we find only the two forms  $\Delta\Delta\text{RRRR}$  (shown in Fig. 1) and  $\Lambda\Lambda\text{SSSS}$ . In the  $\Delta\Delta$  configuration shown in Fig. 5, all four ligands exhibit the  $\lambda$  conformation, which causes the methyl groups to be equatorial.

The four pyridine rings are all virtually planar, with no atom deviating from its least-squares plane by more than  $3\sigma$ . The angle between the planes of the pyridine rings attached to a given metal atom is  $53^\circ$  for Cr(1) and  $51^\circ$  for Cr(2), very similar to the values of 52 and  $50^\circ$  in 1 [20]. Consequently, the A and D rings and the B and C rings are nearly parallel, the angle between the A and D rings being  $12^\circ$  while that between B and C is  $8^\circ$ . The chelate N–N 'bite' distance in the four ligands is in the range 2.593(8) to 2.643(8) Å. The molecular geometries of the four ligands, which are tabulated in Table V, are substantially similar. The C–C bond lengths to the methyl group [C(2)–C(3')] in all four ligands are unreliable because of the high librational motion associated with the methyl groups; this effect is particularly pronounced in the D ring. The averaged ligand dimensions are shown in Table V, and are comparable with those reported by Larsen and Hansen [20]; a view of one ligand is given in Fig. 7.

There is extensive hydrogen bonding in this structure. All of the amine nitrogen atoms form N–H $\cdots$ Br hydrogen bonds to the anions, with NA' and NC' forming one such hydrogen bond and the other two forming two each. The other potential donor in the cation, the bridging OH group, participates in

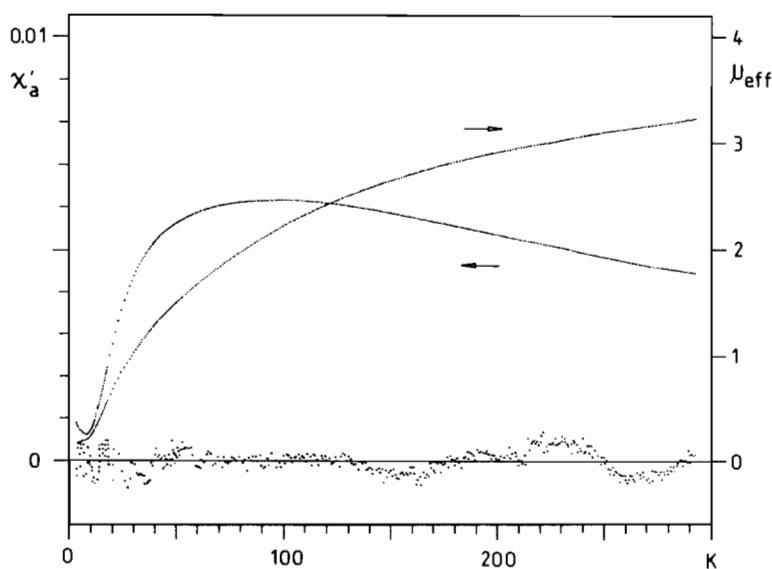


Fig. 8. Magnetic susceptibility per chromium (left scale, cgs units) and effective magnetic moment (right scale, Bohr magnetons) of  $[(2\text{-picetam})_4\text{Cr}_2(\text{OH})(\text{O})]\text{Br}_3 \cdot 5\text{H}_2\text{O}$ . The lower, almost random distribution of dots around the abscissa represents the corresponding values of  $(\chi_{\text{obs}} - \chi_{\text{calc}}) \times 100$ , where  $\chi_{\text{calc}}$  refers to the parameters of model 3 in Table VI.



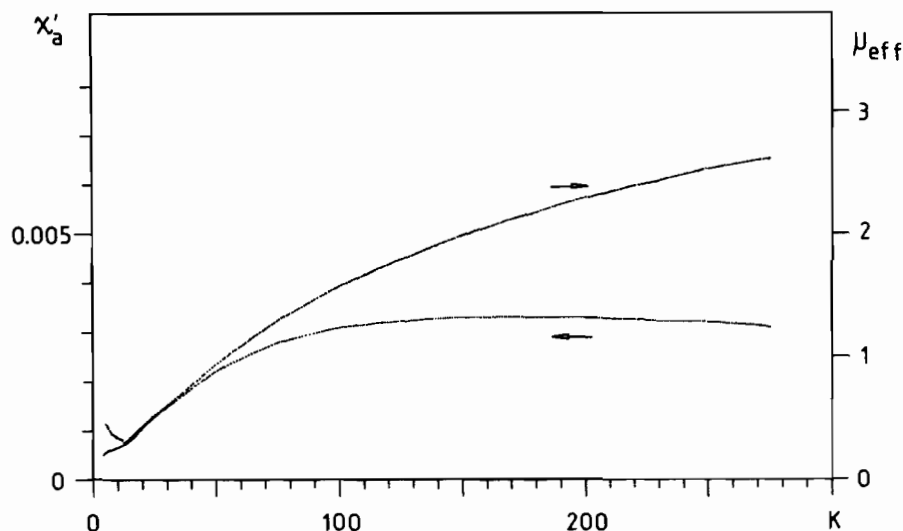


Fig. 9. Magnetic susceptibility and effective magnetic moment of  $[(2\text{-picetam})_2\text{Cr(O)}]_2\text{Cl}_2 \cdot 8\text{H}_2\text{O}$ , plotted as in Fig. 8.

hydrogen bonding to a water molecule, as does amine atom  $\text{NA}'$ . The water molecules are probably also extensively hydrogen bonded to each other and to anions, but since we were unable to locate the hydrogen atoms associated with these solvents molecules no detailed discussion of these interactions is justified.

#### Magnetic Properties

The average magnetic susceptibilities and effective moments of  $[(2\text{-picetam})_2\text{Cr(OH)(O)Cr(2-picetam)}_2]\text{Br}_3 \cdot 5\text{H}_2\text{O}$  and  $[(2\text{-picetam})_2\text{CrQ}]_2\text{Cl}_2 \cdot 8\text{H}_2\text{O}$  as functions of temperature are shown in Figs. 8 and 9. The susceptibility data were fitted to the expression

$$\chi'_A = -\frac{N}{H} \frac{\sum_i \left( \frac{\partial E_i}{\partial H} \right) e^{-E_i/kT}}{\sum_i e^{-E_i/kT}} \quad (1)$$

where  $E_i$  are the energies of the 16 components of the ground state manifold, by minimization of

$$\sum_i (\chi_i^{\text{obs}} - \chi'_A)^2 / \left\{ \sigma^2(\chi) + \left( \frac{\partial \chi}{\partial T} \right)^2 \sigma^2(T) \right\} \quad (2)$$

The fitting was accomplished with use of three different models for the exchange Hamiltonian. Model 1 assumed the simple Heisenberg Hamiltonian

$$H = J \cdot \mathbf{S}_1 \cdot \mathbf{S}_2 \quad (3)$$

Model 2 includes a biquadratic exchange term according to

TABLE VI. Parameters Derived from Magnetic Susceptibility Data for  $[(2\text{-picetam})_2\text{Cr(OH)(O)Cr(2-picetam)}_2]\text{Br}_3 \cdot 5\text{H}_2\text{O}$ .

Parameter	Model 1 <sup>a</sup>	Model 2	Model 3
$J$ ( $\text{cm}^{-1}$ )	45.84(4)	48.7(1)	—
$j$ ( $\text{cm}^{-1}$ )	—	-0.41(1)	—
$E(1)$ ( $\text{cm}^{-1}$ )	45.84(4)	46.0(1) <sup>b</sup>	46.45(2)
$E(2)$ ( $\text{cm}^{-1}$ )	137.5(1) <sup>b</sup>	140.6(3) <sup>b</sup>	139.38(9)
$E(3)$ ( $\text{cm}^{-1}$ )	275.0(2) <sup>b</sup>	288.5(6) <sup>b</sup>	291.8(3)
$g$	1.910(2)	1.955(2)	1.945(1)
var/f	6.78	2.01	0.71
% monomer	0.185(4)	0.216(2)	0.193(2)

<sup>a</sup>See text for description of the models. <sup>b</sup>Calculated from the derived parameters; see text.

$$H = J \cdot \mathbf{S}_1 \cdot \mathbf{S}_2 + j(\mathbf{S}_1 \cdot \mathbf{S}_2)^2 \quad (4)$$

Finally, Model 3 assumed independent energies of the triplet, quintet and septet states; and it merely assumed, as do the earlier models, absence of any zero-field splitting within these levels and an isotropic Zeeman effect. Further details concerning the fitting procedure can be found elsewhere [1].

The results of the data fitting for the  $\mu$ -oxo- $\mu$ -hydroxo complex (2) are displayed in Table VI. While the data are reasonably well described by the simple Van Vleck model, it is apparent that inclusion of the biquadratic exchange term (model 2) markedly improves the fit, lowering the variance/degree of freedom (var/f) from 6.78 to 2.01. Moreover, inclusion of the additional variable in

model 3 leads to a further significant improvement,  $\text{var}/f$  being reduced to 0.71. However, from all of these models it is apparent that the  $\mu$ -oxo- $\mu$ -hydroxo complex (2) has a singlet ground state with a triplet state lying approximately  $46 \text{ cm}^{-1}$  higher in energy.

Attempts to fit the magnetic susceptibility data of the di- $\mu$ -oxo complex (3) were less successful. As can be seen in Fig. 9, the data exhibit a broad maximum centered near 170 K indicative of a strong antiferromagnetic interaction. Attempts to apply any of the magnetic models described above, however, invariably yielded unreasonably small values of  $g$  while apparently fitting the observed data. This phenomenon could be due to an incorrect assumption on our part concerning the molecular weight of the sample, but is more probably due to the presence of small amounts of some other antiferromagnetically-coupled material; in the present case, of course, the presence of a small quantity of the  $\mu$ -oxo- $\mu$ -hydroxo complex is not unlikely. It is also noteworthy in this connection that the magnetic susceptibility of chromium(III) dimers is expected to be relatively insensitive to small changes in  $J$  when (as in the present case)  $J$  is large. The best fits using any of the three models gave values of  $E(1)$  of approximately  $83 \text{ cm}^{-1}$ , so we may safely deduce that the triplet energy in the di- $\mu$ -oxo complex is  $83 \pm 5 \text{ cm}^{-1}$  above the singlet ground state. This observation, along with the preliminary structural data for R and  $\phi$  [30], is entirely consistent with the Glerup-Hodgson-Pedersen GHP [17] magnetic model, from which we calculate a  $J$  value of  $80.4 \text{ cm}^{-1}$ .

### Acknowledgements

We are very grateful to Dr. Sine Larsen for making the results of her work available to us before their publication and to Dr. Ole Mønsted for the determination of acid dissociation constants. Acknowledgment is made to the Donors of The Petroleum Research Fund, administered by the American Chemical Society, for the support of this research through grant No. 12128-AC3,6 (to DJH), to the Danish National Science Research Council through grants No. 511-742, 511-3993, and 511-10516 (to EP), to the Scientific Affairs Division, North Atlantic Treaty Organization (NATO) through grant No. 1318 (to DJH and EP), and to the U.S. National Science Foundation for grant No. CHE78-03064 (to DJH).

### References

- 1 K. Michelsen and E. Pedersen, *Acta Chem. Scand.*, **A32**, 847 (1978).
- 2 J. Josephsen and E. Pedersen, *Inorg. Chem.*, **16**, 2534 (1977).
- 3 S. J. Cline, S. Kallosøe, E. Pedersen and D. J. Hodgson, *Inorg. Chem.*, **18**, 796 (1979).
- 4 A. Beutler, H. U. Güdel, T. R. Snellgrove, G. Chapuis, and K. Schenk, *J. Chem. Soc., Dalton Trans.*, 983 (1979).
- 5 K. Kaas, *Acta Cryst.*, **B35**, 596 (1979); 1603 (1979).
- 6 (a) J. Springborg, *Acta Chem. Scand.*, **A32**, 231 (1978). (b) J. Springborg and H. Toftlund, *Acta Chem. Scand.*, **A33**, 31 (1979). (c) F. Christensson, J. Springborg and H. Toftlund, *Acta Chem. Scand.*, **A34**, 317 (1980).
- 7 H. Oki and H. Yoneda, *Inorg. Chem.*, **20**, 3875 (1981).
- 8 W. E. Hatfield, J. J. MacDougall and R. E. Shepherd, *Inorg. Chem.*, **20**, 4216 (1981).
- 9 K. Michelsen, *Acta Chem. Scand.*, **A30**, 521 (1976); **A31**, 429 (1977).
- 10 D. J. Hodgson and E. Pedersen, *Inorg. Chem.*, **19**, 3116 (1980).
- 11 G. Srdanov, R. Herak, D. J. Radanović and D. S. Veselinić, *Inorg. Chim. Acta*, **38**, 37 (1980).
- 12 S. J. Cline, J. Glerup, D. J. Hodgson, G. S. Jensen and E. Pedersen, *Inorg. Chem.*, **20**, 2229 (1981).
- 13 D. J. Hodgson, *Progr. Inorg. Chem.*, **19**, 173 (1975).
- 14 R. P. Scaringe, D. J. Hodgson and W. E. Hatfield, *Trans. Met. Chem.*, **6**, 340 (1981).
- 15 S. J. Cline, D. J. Hodgson, S. Kallosøe, S. Larsen and E. Pedersen, submitted for publication.
- 16 H. U. Güdel and U. Hauser, *J. Solid State Chem.*, **35**, 230 (1980).
- 17 J. Glerup, D. J. Hodgson and E. Pedersen, submitted for publication.
- 18 J. Josephsen and C. E. Schäffer, *Acta Chem. Scand.*, **24**, 2929 (1970). For a detailed discussion of the aqueous equilibria of complexes of these types, see J. Springborg and H. Toftlund, *J. Chem. Soc., Chem. Commun.*, 422 (1975).
- 19 K. Michelsen, *Acta Chem. Scand.*, **A28**, 428 (1974).
- 20 S. Larsen and B. Hansen, *Acta Chem. Scand.*, **A35**, 105 (1981).
- 21 L. Mønsted and O. Mønsted, *Acta Chem. Scand.*, **A30**, 203 (1976).
- 22 W. E. Marsh, T. L. Bowman, C. S. Harris, W. E. Hatfield and D. J. Hodgson, *Inorg. Chem.*, **20**, 3864 (1981).
- 23 P. Main, M. M. Woolfson, M. Declercq and G. Germain, 'MULTAN: A Program for the Automatic Solution of Crystal Structures', University of York, England.
- 24 P. W. R. Corfield, R. J. Doedens and J. A. Ibers, *Inorg. Chem.*, **6**, 197 (1967).
- 25 M. R. Churchill, *Inorg. Chem.*, **12**, 1213 (1973).
- 26 S. F. Mason, *Rev. Chem. Soc.*, **17**, 20 (1963).
- 27 This value is calculated from the cell constants obtained from X-ray powder data collected by one of us (E.P.), using the atomic positional parameters given in reference 28. It can be contrasted with the value of 1.803(3) Å given in reference 28, and with that of 1.821(3) Å given in reference 29.
- 28 A. Urushiyama, *Bull. Chem. Soc. Jpn.*, **45**, 2406 (1972).
- 29 M. Yevitz and J. A. Stanko, *J. Am. Chem. Soc.*, **93**, 1512 (1971).
- 30 S. Larsen, private communication. We are very grateful to Dr. Larsen for providing us with a preliminary description of her structural analysis of complex 3.